Atmos. Chem. Phys. Discuss., 8, 5235–5268, 2008
www.atmos-chem-phys-discuss.net/8/5235/2008/

Atmospheric Chemistry and Physics Discussions

A combined particle trap/HTDMA hygroscopicity study of mixed inorganic/organic aerosol particles

A. A. Zardini[1], S. Sjogren[2], C. Marcolli[1], U. K. Krieger[1], M. Gysel[2], E. Weingartner[2], U. Baltensperger[2], and T. Peter[1]

[1]Institute for Atmospheric and Climate Science, ETH, CH-8092 Zurich, Switzerland
[2]Laboratory of Atmospheric Chemistry, Paul Scherrer Institut, CH-5232 Villigen, Switzerland

Received: 22 January 2008 – Accepted: 12 February 2008 – Published: 12 March 2008

Correspondence to: U. K. Krieger (ulrich.krieger@env.ethz.ch)

Published by Copernicus Publications on behalf of the European Geosciences Union.

Abstract

Atmospheric aerosols are often mixtures of inorganic and organic material. Organics can represent a large fraction of the total aerosol mass and are comprised of water-soluble and insoluble compounds. Increasing attention was paid in the last decade to the capability of mixed inorganic/organic aerosol particles to take up water (hygroscopicity). We performed hygroscopicity measurements of internally mixed particles containing ammonium sulfate and carboxylic acids (citric, glutaric, adipic acid) in parallel with an electrodynamic balance (EDB) and a hygroscopicity tandem differential mobility analyzer (HTDMA). The organic compounds were chosen to represent three distinct physical states. During hygroscopicity cycles covering hydration and dehydration measured by the EDB and the HTDMA, pure citric acid remained always liquid, adipic acid remained always solid, while glutaric acid could be either. We show that the hygroscopicity of mixtures of the above compounds is well described by the Zdanovskii-Stokes-Robinson (ZSR) relationship as long as the two-component particle is completely liquid in the ammonium sulfate/citric acid and in the ammonium sulfate/glutaric acid cases. However, we observe significant discrepancies compared to what is expected from bulk thermodynamics when a solid component is present. We explain this in terms of a complex morphology resulting from the crystallization process leading to veins, pores, and grain boundaries which allow for water sorption in excess of bulk thermodynamic predictions caused by the inverse Kelvin effect on concave surfaces.

1 Introduction

Atmospheric aerosols influence the climate directly through scattering and absorption of radiation, and indirectly through modification of clouds properties. The climate forcing resulting from these aerosol effects is still subject to large uncertainties (IPCC, 2007). Organic material accounts for 20% to 50% in total fine aerosol mass at continental mid-latitudes and for as much as 90% in tropical forested areas (Kanakidou

et al., 2005). Organics in the condensed phase comprise a large variety of chemical compounds (Rogge et al., 1993). Although large uncertainty remains concerning the detailed composition, it is established that a considerable fraction of the organic aerosol is water-soluble, thus contributing to aerosol hygroscopicity (Choi and Chan, 2002; Saxena et al., 1995). Moreover, organics are typically found to be internally mixed with inorganic compounds (Middlebrook et al., 1998; Murphy et al., 2006), and may therefore influence the water uptake and phase changes of the inorganic aerosol fraction (Saxena et al., 1995; Cruz and Pandis, 2000; Dick et al., 2000).

Considering the complex composition of atmospheric aerosols with thousands of different compounds, Marcolli et al. (2004) suggested that the physical state of the organic aerosol fraction is typically liquid (or amorphous solid). The determination of the physical state (liquid or crystalline) and the amount of water present in the condensed matter is crucial to assess the aerosol impact on climate and atmospheric chemistry.

Chemical interactions between the inorganic and organic species may lead to a decrease of the deliquescence relative humidity of the inorganic component, or even to water uptake by the aerosol particle at any relative humidity (Braban and Abbatt, 2004; Choi and Chan, 2002). Alternatively, a liquid/liquid phase separation into a predominantly organic and an aqueous inorganic phase may occur without change of the inorganic salt deliquescence relative humidity (Marcolli and Krieger, 2006).

Moreover, mass transfer limitations between gas and particle phase play a role in water uptake kinetics, increasing the time required by the particles to equilibrate with ambient relative humidity (Chan and Chan, 2005; Sjogren et al., 2007). We observed slow water uptake for mixed inorganic/organic particles in HTDMA measurements and hypothesized that complex morphology of mixed solid/liquid aerosol particles is responsible for this behavior (Sjogren et al., 2007).

The method of choice often used to predict the hygroscopic behavior of multicomponent particles is the Zdanovskii-Stokes-Robinson's approach (Zdanovskii, 1948; Stokes and Robinson, 1966). It assumes that there are no interactions between the different components of the mixed solution particle, and therefore the total water up-

take is simply the sum of the individual uptakes by the single components. While this method proved to be valid for many systems, discrepancies still remain for other mixtures, e.g. involving pinonic acid (Cruz and Pandis, 2000), succinic acid (Svenningsson et al., 2006), or adipic acid (Sjogren et al., 2007, and this study).

As pointed out by Fuzzi et al. (2006), despite the remarkable advances in recent years, physicochemical properties such as the hygroscopicity of organic particles need further investigation and improvements of measurement techniques.

This study sheds more light on the problem by investigating the hygroscopicity (in terms of the growth factor) and morphologies (including phase changes) of mixed inorganic/organic particles made of ammonium sulfate as inorganic component and either citric, glutaric, or adipic acid as organic component. These organic compounds are typically found in secondary or aged primary organic aerosols. Measurements are performed in parallel with an electrodynamic balance and an HTDMA instrument, and results are compared with literature data and/or bulk thermodynamics. A comparison of the measured growth factors with the Zdanovskii-Stokes-Robinson approach is also shown. Characteristic deviations from ideality are identified and discussed.

2 Experiment and method

2.1 Electrodynamic balance

The basic experimental setup has been described previously (Krieger et al., 2000). Briefly, an electrically charged particle (typically 5–25 μm in radius) is levitated in an electrodynamic balance (Davis et al., 1990), see a schematic of the setup in Fig. 1. The balance is hosted within a three wall glass chamber with a cooling agent flowing between the inner walls and an insulation vacuum between the outer walls. A constant flow (typically 30 sccm) of an N_2/H_2O mixture with a controlled H_2O partial pressure is pumped continuously through the chamber at a constant total pressure adjustable between 200 and 1000 mbar.

The temperature can be varied between 330 K and 160 K with a precision better than 0.1 K and an accuracy of ±0.5 K. The relative humidity (RH) in the chamber is set by adjusting the N_2/H_2O ratio, using automatic mass flow controllers. The relative humidity is registered by a capacitive thin film sensor that is mounted in close vicinity (<10 mm) of the levitated particle. The sensor was calibrated directly in the electrodynamic balance using the deliquescence relative humidity of different salts. Its accuracy is ±1.5% RH between 10% and 90% RH.

A single-particle generator (Hewlett-Packard 51633A ink jet cartridge) is used to inject a liquid particle from solutions prepared by mass percent with MilliQ water using an analytical balance and analytical grade reagents with purities of 99% or higher. Two collinear laser beams illuminate the particle from below (HeNe@633 nm, Ar^+@488 nm).

To characterize the particle three different, independent methods are employed. First, we use the video image of the particle on CCD detector 1 and an automatic feedback loop to adjust the DC-voltage for compensating the gravitational force (Richardson, 1990). A change in DC voltage is therefore a direct measure of the mass change, allowing to calculate a radius change when the density of the particle is known or can be estimated.

Second, the two-dimensional angular scattering pattern is recorded with CCD detector 2 by measuring the elastically scattered light from both lasers over observation angles ranging from 78° to 101°. If the particle is liquid, and therefore of spherical shape, the scattering pattern is regular, with the mean distance between fringes being a good measure of the radius of the particle, almost independent of its refractive index (Davis and Periasamy, 1985).

Third, we use a photomultiplier with a relatively small conical detection angle (approximately 0.2° half angle) to measure the scattering intensity at 90° to the incident beam, and feeding this signal to an analog lock-in amplifier (Stanford Research System model SR510) to measure the intensity fluctuations at the frequency of the AC field of the electrodynamic trap (with a 10 Hz ENBW). This yields the root mean squared

deviation (RMSD) from the intensity mean of the scattered intensity, which can be associated with the particle morphology: low values for spherical homogeneous particle and high values for crystalline shape (see Videen, 1997, and Krieger and Braun, 2001, for details).

2.2 Hygroscopicity tandem differential mobility analyzer

The HTDMA was used to determine the hygroscopic growth, i.e., the change of aerosol particles diameter due to the uptake of water. The experimental set up has been fully described before (Weingartner et al., 2002; Gysel et al., 2004; Sjogren et al., 2007). The compounds were dissolved in MilliQ water (typically 0.1–1 g/L) and all solute appeared completely dissolved at visual inspection. The particles were generated using an atomizer (TSI 3076) operated with purified compressed air. It is assumed that the resulting aerosol was internally mixed with the same mass ratio as in the solution as no broadening of the growth factor distributions from the HTDMA could be detected while switching from the pure ammonium sulfate to the mixtures. The particles first entered a silica gel diffusion dryer (flow rate: 300 sccm) in order to dry the sample to RH<10% at 298 K. The dry aerosol is subsequently brought to charge equilibrium using a bipolar diffusion charger (^{85}Kr) and then fed into the first differential mobility analyzer (DMA), where a narrow size cut of the dry aerosol (D_0=100 nm) is selected. The particle diameter resulting after equilibration at a well defined higher RH (20 to 25 s residence time) is then measured using a second DMA and a condensation particle counter (CPC; TSI CPC 3022A). The exact D_0 is determined by keeping the particles exposed to dry conditions (RH≤10%), in which case no size change occurs. With this apparatus, hygroscopic growth of particles with diameters between 20 and 250 nm can be determined in the temperature range of 253–303 K and humidity range of 10% to 95% RH with an accuracy of $\Delta T = \pm 0.1$ K and ΔRH=±1.5% at 95% RH. The hygroscopic growth factor is determined with a precision of ±0.01 (at D_0) and ±0.03 (at RH=80%) (Sjogren et al., 2007).

Since the initial particle size selected with the HTDMA is D=100 nm, the Kelvin effect

plays a role in limiting the water uptake due to high curvature of smaller droplets. For solution droplets with surface tension of pure water the growth factors measured with the HTDMA are therefore expected to be 1–2% lower than those calulated with the EDB and bulk samples. No correction for this effect was applied.

2.3 Method

During our measurements, particles are exposed to hygroscopicity cycles with relative humidities increasing from RH≈10% to RH≈85% and again decreasing (at a typical rate dRH/dt≈10%/h for the EDB), while pressure and temperature are kept constant at $T \approx 291$ K and $P \approx 600$ torr for the EDB, $T \approx 292$ K and atmospheric pressure for the HTDMA.

Particle mass (for the EDB) and mobility diameter (for the HTDMA) are monitored and the results are presented in so-called humidograms, where the mass growth factor g is plotted versus RH. In order to do so, the size change measured with the HTDMA is converted to a mass change via

$$g(\mathrm{RH}) = \frac{m(\mathrm{RH})}{m_0} = 1 + \left(G^3(\mathrm{RH}) - 1\right)\frac{\rho_w}{\rho_0}, \quad (1)$$

where m(RH) is the mass of the particle depending on relative humidity, m_0 and ρ_0 are the initial particle mass and density at dry conditions, ρ_w is the density of water, and $G = D/D_0$ is the size growth factor. This equation assumes that the density of the sample is linearly dependent on the volume mixing ratio of the solute and the absorbed water (i.e. that the volume occupied by a single solute molecule is independent from the presence of the water molecules). It is further assumed that the measured mobility diameter is equal to the volume equivalent diameter, which is the case for a droplet with elevated water content, but might not be fulfilled for non-spherical dry particles due to dynamic shape factors being different from 1.0. As no significant deviations from sphericity at dry conditions were observed, the use of the above equation is justified.

The EDB technique measures relative mass changes as explained in the experimental section. Therefore, it is necessary to identify a reference state to calculate the mass growth factor. One option can be the choice of the voltage at very dry conditions, typically $RH = 10\%$, as normalizing factor, in which case $g(10\%) = 1$. However, it is often difficult to assure that at a low RH the particle is completely free of water (Peng et al., 2001). In the present work, following previous hygroscopicity studies (e.g. Choi and Chan, 2002), we measured the water activity of the compounds listed in Table 1 and their mixtures in various concentrations using the AquaLab water activity meter (Model 3TE, Decagon Devices). The EDB voltage was then normalized to match the bulk data at RH≈80%.

For two-component particles as the ones studied in this paper, the Zdanovskii-Stokes-Robinson (ZSR) relation (Zdanovskii, 1948; Stokes and Robinson, 1966) can be simply written as:

$$g(\mathrm{RH}) = g_1(\mathrm{RH})w_1 + g_2(\mathrm{RH})w_2, \quad (2)$$

where g is the total mass growth factor of the two-component particle as a function of relative humidity, g_1 is the ammonium sulfate mass growth factor calculated with the thermodynamic model proposed by Clegg et al. (1998) (available at: http://mae.ucdavis.edu/wexler/aim.htm/), g_2 is the mass growth factor of pure organic particles measured with the EDB, and w_1 and w_2 are the mass fractions of the two components in the dry particle. The ZSR relation assumes independent (i.e. linearly additive) hygroscopic behavior of the different components in the mixed particle.

3 Results

3.1 Ammonium sulfate and citric acid (AS/CA)

Hygroscopicity measurements of particles made of pure ammonium sulfate, pure citric acid, and mixtures of the two with different mixing ratios (AS:CA=4:1, 2:1, 1:1 mo-

lar ratios) are performed with the EDB and HTDMA. The results are compared with literature, bulk data and ZSR predictions in Fig. 2.

The uppermost panel shows the humidogram of pure ammonium sulfate particles at ambient temperature. The hygroscopicity of a pure ammonium sulfate particle is well known: solid ammonium sulfate exposed to increasing RH initially does not take up water until it exhibits discontinuity at RH≈80%, the thermodynamically determined deliquescence relative humidity (DRH), where the crystalline to liquid phase transition occurs. After deliquescence, the particle takes up or releases water gradually upon RH changes without undergoing a phase change at the DRH. Rather, it remains in a supersaturated metastable state at intermediate RH and recrystallizes only at relative humidities below RH=35%–40% The latter is termed efflorescence relative humidity (ERH), although it is kinetically determined, depending on a nucleation event and therefore not corresponding to a fixed value. The measured growth factors are in agreement with the thermodynamic model by Clegg et al. (1998) (see Fig. 2).

In contrast, pure citric acid particles are always in liquid state during our experiments as shown in the lowermost panel of Fig. 2: they take up or release water gradually without phase changes in the whole range of relative humidities studied here. EDB and HTDMA measurements of this study are in reasonable agreement with EDB and bulk measurements of previous studies (Levien, 1955; Apelblat et al., 1995; Peng et al., 2001). Note that citric acid retains some water even at low RH ($g > 1$ for RH≈10%).

Our pure citric acid cycles measured with the EDB together with bulk points were fitted to obtain the following parametrization for the pure citric acid growth factor: $g_2(RH)=1.27774 - 5.705\ RH + 41.8\ RH^2 - 143.806\ RH^3 + 256.938\ RH^4 - 227.958\ RH^5 + 79.7803\ RH^6$ for RH between 10% and 90%. This formula is used in Eq. 2 to calculate the ZSR predictions for the mixtures. In the AS:CA=4:1 case, panel (b) of Fig. 2, the particles start to take up water well before the full deliquescence of AS at RH≈80%. After passing the 80% RH, the particles are in fully liquid state and absorb or desorb water according to RH changes until AS effloresces at ERH around 35% (HTDMA) or 38% (EDB). The red line results from the ZSR calculations as in Eq. 2, assuming full

dissolution of the components for the dehydration branch, and no dissolution of AS up to its deliquescence point for the hydration branch. This underestimates the measured water uptake during hydration, indicating that in fact also AS starts dissolving before full deliquescence and takes up some water. For the dehydration branch, results from both techniques, EDB and HTDMA, are in agreement with the ZSR prediction (within 10%).

Panel (c) of Fig. 2 shows the hygroscopicity cycle of AS/CA particles, 2:1 mixture. Here the measurements from EDB and HTDMA differ: the single particle in the EDB exhibits clearly separated hydration/dehydration branches, while the HTDMA does not. After injection of the particle into the EDB, a solid inclusion forms and dissolves completely at RH≈76% during moistening. The water uptake before full dissolution is consistent with the measured water activity of the correspondent bulk solution and indicate the capability of a hydrophylic organic to lower the deliquescence point of ammonium sulfate. Upon subsequent drying the particle remains liquid and it cannot be forced to effloresce even at RH as low as 10%.

The presence of a solid inclusion, its deliquescence and the absence of efflorescence are confirmed by the light fluctuation and radius signals in the uppermost and middle panels of Fig. 3: at the beginning of the hygroscopicity cycle the RMSD datapoints are typical of a liquid particle with a solid inclusion and decrease to values typical of a homogeneous, spherical particle (i.e., liquid) at t=20 ks. Also, the algorithm for calculating the particle radius works properly after t=20 ks, providing indirect evidence for spherical shape with a homogeneous particle phase. Nevertheless, even before t=20 ks the radius datapoints provide a rough estimate of the radius (increasing monotoneously from r≈4.2 μm at t=0 s to r≈4.6 μm at t=20 ks), indicating an almost spherical, but non-homogeneous particle taking up water with increasing RH.

The physical reason for partial efflorescence only occurring at initial particle injection into the trap is not clear. The crystallization must be attributed to the ammonium sulfate fraction (since citric acid is always in liquid state in our experiments) and it could be a consequence of the precipitous evaporation experienced by the particle immediately

after injection into the EDB. In fact, the liquid droplet of about 50 μm diameter produced by the injection device shrinks suddenly (few ms) to the particle size in thermodynamic equilibrium (radius ≈5 μm) with ambient conditions. The fast evaporation must induce a cooling of the particle and a strong, rapidly changing concentration gradient within the particle which in turn could be responsible for the AS crystallization. The reproducibility of partial efflorescence of the particle upon injection but not in subsequent hygroscopicity cycles was tested and confirmed by several injections in the EDB. The particles in the HTDMA, instead, are always liquid and gradually absorb or desorb water at any given RH.

Panel (d) of Fig. 2 shows the hygroscopicity cycle of AS/CA, 1:1 molar ratio. No efflorescence/deliquescence occurrence is detected with either technique, i.e., the particles remain liquid and gradually absorb/desorb water. EDB and HTDMA measurements agree with literature data and with the ZSR curve.

To summarize, the hygroscopicity of the two-component system ammonium sulfate/citric acid is characterized by a distinct, reduced, and completely absent hysteresis when decreasing the molar mixing ratio from 4:1 via 2:1 to 1:1. In the 2:1 case both DRH and ERH are reduced, the ERH potentially to such an extent that crystallization does not occur at the lowest RH reached in the HTDMA and the EDB, but only occurs for initial particle injection into the EDB. For the dehydration branches of the fully liquid particles, EDB and HTDMA measurements are in good agreement and the ZSR approach provides a suitable description. For the hydration branches, the ZSR approach assuming no dissolution of AS before full deliquescence underestimates the observed water uptake, indicating that AS dissolves partially in aqueous citric acid at low RH.

3.2 Ammonium sulfate and glutaric acid (AS/GA)

Hygroscopicity cycles of pure glutaric acid and mixed ammonium sulfate/glutaric acid (AS:GA=1:1 molar ratio) particles were performed with the EDB. HTDMA cycles were also measured, but they are not shown because no reliable results could be achieved due to substantial evaporative shrinking of the particles within the instrument. Such

evaporation artifacts in HTDMA instruments have previously been reported by Prenni et al. (2003), as well as Cruz and Pandis (2000) for submicrometer size glutaric acid particles.

Pure glutaric acid exhibits hysteresis with distinct deliquescence and efflorescence as shown in Fig. 4. The DRH of glutaric acid has been determined by several groups: Brooks et al. (2002): DRH=87.5%; Wise et al. (2003): DRH=88.9%; Marcolli et al. (2004) DRH=88.2% (all bulk measurements at 298 K). Pant et al. (2004) found DRH≈89% by using a reflected-light microscope technique. In this study we find DRH≈90%, a slightly higher value likely due to the temperature dependence of glutaric acid DRH: unlike ammonium sulfate, the solubility of glutaric acid is strongly temperature dependent.

HTDMA data from Cruz and Pandis (2000) strongly underestimate the amount of water uptake at deliquescence (DRH≈85%). In addition, a size decrease at RH≈50% possibly caused by structural rearrangements inside the particle or shrinking due to evaporation was observed. The DRH determined with EDB at 298 K by Peng et al. (2001) is 83.5%≤DRH≤85%. A reason for this lower value might be the presence of impurities in the glutaric acid used for their experiment.

In contrast, the efflorescence behavior is characterized by a low degree of reproducibility. The EDB cycles in Fig. 4, indicate efflorescence at RH≈43% (this study) and between 29% and 33% (Peng et al., 2001). However, during consecutive cycles that we performed with another particle shown in Fig. 5, efflorescence occurred at RH between 25% and 35% as a multi-step process, with a first mass decrease and a subsequent gradual water release (red and green curves), or as a gradual water release (black curve). In contrast, the analysis of scattered light fluctuations reveals that the phase change from liquid to solid is a well defined efflorescence: during each cycle the particle solidifies at a well defined RH as indicated in Fig. 6, where the experimental raw data corresponding to the black curve in Fig. 5 are plotted. It is evident from the RMSD data (uppermost panel) that the particle undergoes two phase changes, one from solid to liquid at t≈32 ks (RH≈90.5%), and one from liquid to solid at t≈55 ks (RH≈18%).

This reveals the physicochemical behavior of glutaric acid to be very complex and more than one experimental technique has to be invoked to fully characterize it.

Figure 7 shows a complete hygroscopicity cycle of an ammonium sulfate/glutaric acid particle with 1:1 molar ratio of the mixture together with results from literature. The particle is completely crystalline and does not take up water until it fully deliquesces at DRH≈77.5%, while the efflorescence occurs at ERH≈32%. The molar ratio chosen is very close to the eutonic composition of the ammonium sulfate/glutaric acid solution (see Pant et al., 2004), thus resulting in a single step and well defined deliquescence. Our work and that from Choi and Chan (2002) show a lower water uptake than ZSR predictions in the metastable region at dry conditions, while the growth factor at DRH matches the ZSR curve perfectly. Pant et al. (2004) investigated in detail the DRH and ERH occurrence for the AS/GA system. For the AS:GA=1:1 mixture they found DRH≈78% and ERH≈28%, while DRH=76.7% was observed in bulk measurements by Wise et al. (2003). These results are in good agreement with ours.

3.3 Ammonium sulfate and adipic acid (AS/AA)

Pure adipic acid particles remain crystalline and do not deliquesce at relative humidities up to 99%, therefore adipic acid is generally regarded as an inert aerosol component (Sjogren et al., 2007; Hameri et al., 2002). We already presented hygroscopic measurements of mixed ammonium sulfate/adipic acid particles in Sjogren et al. (2007). In that study the kinetics and morphology of the system was investigated: we proposed that adipic acid, when present in major fractions stays always in solid state, as verified with light fluctuation measurements in the EDB, encapsulating some of the inorganic species residing in the crystalline organic veins and pores.

The water uptake rate of the inorganic solution is then probably limited by solid phase diffusion (water through solid adipic acid). The conclusion was that sufficient residence time in the HTDMA is required for such systems to equilibrate, or measurements will be misleading.

Here we report on two cases of mixed AS/AA particles consisting mostly of ammonium sulfate (AS:AA=2:1.1, molar ratio) or adipic acid (AS:AA=1:3.3, molar ratio), see Fig. 8. The 2:1.1 case (upper panel) resembles the behavior of pure ammonium sulfate of Fig. 2, uppermost panel, except for the lower growth factors in the dehydration branch due to the presence of the inert adipic acid, in agreement with ZSR predictions. However, in the 1:3.3 case (lower panel) the hygroscopic cycle strongly differs from the ZSR prediction in both hydration and dehydration branches of the EDB measurements. A pre-deliquescence water uptake starting at RH≈45% is followed by full deliquescence of ammonium sulfate at RH≈80%. Upon dehydration, more water than predicted by the ZSR approach is retained by the particle until the efflorescence of ammonium sulfate occurs at RH≈35%. The pre-deliquescence water uptake is not detected by the HTDMA (blue triangles in lower panel of Fig. 8), indicating no change in total particle volume and suggesting that the water must be taken up in the complex particle inner structure as a consequence of Kelvin effect on concave surfaces. In particular, the dark yellow curve in the lower panel indicates a pre-deliquescence water uptake which is followed by a water loss despite growing RH - presumably due to the collapse of some pores and veins after partial dissolution of ammonium sulfate leading to larger pore diameters and a decreased Kelvin effect. This morphology change would cause part of the water taken up during pre-deliquescence to be released again by the particle. Consecutive cycles made on several particles reproducibly show such a complex pre-deliquescence behavior of varying magnitude with water uptakes of 3–19% in mass starting at RH between 43% and 53%. Table 2 summarizes the EDB measurements for the AS:AA=1:3.3 system.

We think that the reproducibly varying pre-deliquescence and deliquescence are a consequence of the complex morphology of the adipic acid matrix possessing veins and pores that enhance water uptake and enclosures that reduce it. Also, the RH at full deliquescence, which shows a variability slightly above the measurement error, may be influenced by the particle morphology (see detailed explanation in the discussion section). None of the other investigated particles displays such a behavior.

We investigated whether the pre-deliquescence is a reversible process with respect

to relative humidity changes. Figure 9 shows the temporal evolution of two consecutive incomplete cycles where RH, starting from less than 10%, is increased to 70% and then lowered again to reach very dry ambient conditions. The scattered light intensity fluctuations (RMSD, orange symbols) are in opposite phase with the mass changes, indicating that the shape of the particle is getting more spherical while mass and RH are increasing (black and red curves). RMSD values are typical of crystalline particles during the whole experiment. This is consistent with a water uptake which fills the pores of the solid particle because of the Kelvin effect on concave surfaces, conferring a more spherical shape and possibly a more homogeneous refractive index. By decreasing the relative humidity, the water evaporates, pores and cavities are depleted of water and the particle turns back to a more irregular crystalline shape. The process is hence reversible with respect to relative humidity changes.

4 Discussion

We have studied three two-component inorganic/organic systems representing three distinct physical states that also occur in atmospheric aerosols:

- Liquid particles;
- Liquid/Solid particles;
- Solid particles.

In this study liquid particles appeared to remain always homogeneously mixed (i.e. liquid-liquid phase separations were not observed). The EDB experiments indicate that mixed phase particles, with liquid and solid phases, contain a conglomerate of nanocrystals with irregular shapes, with cracks, pores and veins. These pores and veins between the crystals fill with aqueous solution, depending on relative humidity. The water uptake in such pores and veins is enhanced compared to the one of a flat surface or the convex particle surface (Camuffo, 1998). As we argued in Sjogren et al.

(2007), the enhancement depends on the vein diameter, determining the concavity of the liquid surface at the opening of the vein, and results in a Kelvin effect that is inverse compared to that of a convex liquid droplet.

The ambient relative humidity in equilibrium with a micropore of radius r filled with aqueous solution has been calculated by Thomson, later Lord Kelvin (Thomson, 1871):

$$\mathrm{RH}(r) = a_w \exp\left(-\frac{2\sigma V_m}{r\mathcal{R}T}\right), \quad (3)$$

where a_w is the water activity (required when applying the equation to aqueous solutions), σ is the surface tension of the solution, V_m is the molar volume of water and $\mathcal{R}$ the gas constant. The same effect may lead to water uptake prior to deliquescence also for solid particles consisting of conglomerates of nanocrystals. Below, we will discuss the hygroscopicity of the different phase states for the systems investigated this study.

4.1 Liquid

When both components of the particle are in the liquid state, the hygroscopicity can be adequately explained by the ZSR approach. The water uptake of the particle is the sum of the water uptakes of the single components. Our EDB and HTDMA measurements agree with the ZSR predictions and with bulk measurements (see AS:CA=4:1, 2:1, 1:1, and AS:GA=2:1 cycles in Fig. 2, dehydration branches). Applicability of ZSR suggests that the hygroscopic behavior of the different components in the mixed particle may indeed assumed to be linearly additive.

4.2 Solid/liquid

For the mixed phase cases of AS:CA=4:1 and AS:CA=2:1 (see Fig. 2, hydration branches), with AS being the solid phase, we do not know the detailed composition of the solution in the particle during the hydration before the deliquescence of AS.

Hence, the ZSR approach can not be applied without further assumptions. Application of ZSR with the assumption that AS is present as an inert mass before it deliquesces (being CA the only responsible for water uptake) underestimates the observed water uptake for AS/CA mixtures. We therefore conclude that AS must be partially dissolved in aqueous citric acid and contributes to water uptake. For the AS:CA 2:1 case, the water uptake before full deliquescence as observed in the EDB is in agreement with bulk data, indicating that morphology effects are minor in this system. In a similar study, Marcolli and Krieger (2006) observed higher water uptake than the bulk measurements for the system AS/PEG400 (solid AS, liquid organic).

The system AS:AA=1:3.3 can be regarded as an extreme case showing discrepancies from ZSR predictions both in the hydration and dehydration branches. In the dehydration branch (solid AA, liquid AS) more water is present than expected by the ZSR predictions. We already explored the possibility that this higher water uptake is due to morphological effects in Sjogren et al. (2007): The Kelvin effect leads to enhanced water uptake during and after full deliquescence. During this process the veins and cavities swell to accommodate the excess water leading to a gradual decrease of the Kelvin effect. Depending on the morphology of the individual particle a part of AS may be enclosed in the AA matrix. This part is only accessible to hygroscopic growth by solid state diffusion of water through the AA matrix. In our experiments enclosed AS will lead to a smaller growth factor compared to the one expected from thermodynamics. Therefore, morphology effects may lead to an enhanced or reduced water uptake. This may also explain the scatter of growth factors shown in Table 2.

Upon drying the swollen veins start shrinking and water is released by the particle until the mechanical resistance against further shrinkage leads to the cavities depletion because the Kelvin effect can no longer be sustained; the mass growth factor decreases to values closer to the one of the ZSR prediction at this RH. Efflorescence may occur by heterogeneous nucleation on the surface of AA at any RH below DRH, either in a series of small steps, or in one or few bigger decreases in mass growth factor as indicated in Table 2.

4.3 Solid

The solid/solid case is realized for the AS/GA system, which shows no water uptake before deliquescence. In contrast, the hydration branch of the AS:AA=1:3.3 mixture exhibits a pre-deliquescence water uptake below the DRH of an AS/AA mixture in the eutonic composition. We attribute this process to morphology effects. In short, there is evidence that the particle behaves like a sponge with partly elastic and partly inelastic properties, taking up the water in various degrees of reversibility. The subsequent paragraphs provide some rough quantitative estimates illuminating the nature of these particles.

For an average RH≈53% between the onset and the maximum of the pre-deliquescence, Eq. 3 yields a vein radius of r=2.6 nm, if we use for σ the value of pure water (σ=72.2 Jm^{-2} at T=290 K), and when we assume that a_w=0.8 for a solution inside the veins. A value of a_w=0.8 corresponds to the water activity of bulk aqueous AS in equilibrium with the crystalline phase, below this value no dissolution is expected. The average growth factor prior to deliquescence is g≈1.1 as shown in Table 2. The total vein length follows simply from the formula for a cylindrical volume and from the density definition: $l_v = m_v/(\rho_v \pi r_v^2)$, where m_v is the mass and ρ_v is the density of the aqueous solution in the vein taken from Semmler et al. (2006).

The optical radius of the particle in the EDB can not be exactly calculated for this particular system because the particle is always non-spherical. Nevertheless, a rough estimate of r≈3 μm can be inferred from the spread radius datapoints like those shown in the middle panel of Fig. 3 before deliquescence. The particle density averaged from the densities of crystalline AS and AA is ρ=1.464 g/cm^3; the absolute mass of the particle and hence of the water uptake, can then easily be calculated considering the 10% relative mass increase estimate. The assumption that the veins are filled with a saturated AS solution results in a vein length of l_v=110 cm which, compared with a 3 μm particle size, has to be taken as evidence for a highly porous morphology of the particle required to accommodate the water.

Following Price (2000), we model the conglomerates of nanocrystals as consisting of grains of semiregular truncated octahedra of diameter (between square faces) D. The volume of a grain is $D^3/2$; the grain has 36 edges, each of length $\sqrt{2}D/4$ and shared with three other grains. The total fractional volume (f) in veins is then $f=(6\pi\sqrt{2})(r_{\mathrm{vein}}/D)^2$. The fractional volume is calculated by dividing the fractional mass of the aqueous solution by its density. A mass growth factor of 1.1 as observed corresponds to a fractional volume of a saturated aqueous AS solution of 0.16. This yields a grain diameter of 34 nm for veins with 2.6 nm radius. This compares well with grain sizes observed in SEM images of dry AS/AA mixtures (Sjogren et al., 2007).

The thermodynamics of the AS/AA system together with the morphology described above leads to a consistent view of the hygroscopic cycles as shown in Fig. 8 and Table 2. During moistening, the particle takes up water into the veins at about 53% RH, without changing the vein size. Subsequently, the vein system may partly collapse leading to water release. At the deliquescence RH the AS dissolves and the veins swell. In comparison to ZSR predictions the water uptake is enhanced, depending on the radius of the veins. This effect becomes smaller the more water is taken up at higher RH. A decreased water uptake compared to ZSR is observed when a fraction of the AS is completely enclosed in the AA matrix. Upon drying water is released and the vein radii shrink again leading to a stronger Kelvin effect. This results in an increasing deviation from the ZSR prediction for the metastable aqueous solution. AS appears to effloresce at any given RH below the DRH either in small compartments of the AA matrix separately leading to a series of small steps in the humidogram, or in one larger step if the veins are interconnected.

5 Conclusions

This combined study aimed at shedding more light on the thermodynamic characterization of mixed inorganic/organic aerosol particles by means of two widely used techniques: the electrodynamic balance and the hygroscopicity tandem differential mobility

analyzer. We focused on three organic acids of atmospheric relevance (citric, glutaric and adipic acid) in mixtures with an inorganic salt (ammonium sulfate). These organics are representative of three different water uptake characteristics. The results show that as long as the two-component particles are fully liquid, the Zdanovskii-Stokes-Robinson relation adequately predicts the water uptake (additivity of the water uptake). Whereas, in the presence of a solid phase (being it inorganic or organic), bulk thermodynamics alone appears to be insufficient to fully characterize the system. This corroborates a previous finding that morphology effects play an important role, resulting in water uptake by two-component particles even at dry ambient conditions. In addition, at higher relative humidities the hygroscopic growth factor may deviate considerably from what is expected from bulk thermodynamics.

Acknowledgements. This work was supported by the National Science Foundation Switzerland (grant n° 200021-100280).

References

Apelblat, A., Dov, M., Wisniak, J., and Zabicky, J.: Osmotic and Activity Coefficients of HO2CCH2C(OH)(CO2H)CH2CO2H (Citric Acid) in Concentrated Aqueous Solutions at Temperatures from 298.15 K to 318.15 K, J. Chem. Thermodynamics, 27, 347–353, 1995.

Braban C. F. and Abbatt, J. P. D.: A study of the phase transition behavior of internally mixed ammonium sulfate – malonic acid aerosols, Atmos. Chem. Phys., 4, 1451–1459, 2004, http://www.atmos-chem-phys.net/4/1451/2004/.

Brooks, S. D., Wise, M. E., Cushing, M., and Tolbert, M. A.: Deliquescence behavior of organic/ammonium sulfate aerosol, Geophys. Res. Lett., 29(19), 1917, 2002.

Camuffo, D.: Condensation–Evaporation cycles in pore and capillary systems according to the Kelvin model, Water, Air, and Soil Pollution, 21, 151–159, 1984.

Chan, C. K., Flagan, R. C., and Seinfeld, J. H.: Water activities of NH4NO3(NH4)2SO4 solutions. Atmos. Environ., 26, 1661–1673, 1992.

Chan, M. N. and Chan, C. K.: Mass transfer effects in hygroscopic measurements of aerosol

particles, Atmos. Chem. Phys., 5, 2703–2712, 2005, http://www.atmos-chem-phys.net/5/2703/2005/.
Choi, M. Y. and Chan, C. K.: The Effects of Organic Species on the Hygroscopic Behaviors of Inorganic Aerosols, Environ. Sci. Technol., 36, 11, 2422–2428, 2002.
Clegg, S. L., Brimblecombe, P., and Wexler, A. S.: A thermodynamic model of the system H+ – NH4+ – SO42 – – NO3 – – H2O at tropospheric temperatures, J. Phys. Chem. A, 102, 2137–2154, 1998.
Cruz, C. N. and Pandis, S. N.: Deliquescence and Hygroscopic Growth of Mixed Inorganic-Organic Atmospheric Aerosol, Environ. Sci. Technol., 34(20), 4313–4319, 2000.
Davis, E. J. and Periasamy, R.: Light-scattering and aerodynamic size measurements for homogeneous and inhomogeneous microspheres, Langmuir, 1, 373–379, 1985.
Davis, E. J., Buehler, M. F., and Ward, T. L.: The double-ring electrodynamic balance for microparticle characterization, Rev. Sci. Instrum., 61, 1281–1288, 1990.
Dick, W. D., Saxena, P., and McMurry, P. H.: Estimation of water uptake by organic compounds in submicron aerosols measured during the Southeastern Aerosol and Visibility Study, J. Geophys. Res., 105(D1), 1471–1479, 2000.
Fuzzi, S., Andreae, M. O., Huebert, B. J., Kulmala, M., Bond, T. C., Boy, M., Doherty, S., J., Guenther, A., Kanakidou, M., Kawamura, K., Kerminen, V M., Lohmann, U., Russell, L. M., and Pöschl, U.: Critical assessment of the current state of scientific knowledge, terminology, and research needs concerning the role of organic aerosols in the atmosphere, climate, and global change, Atmos. Chem. Phys., 6, 2017–2038, 2006, http://www.atmos-chem-phys.net/6/2017/2006/.
Gysel, M., Weingartner, E., Nyeki, S., Paulsen, D., Baltensperger, U., Galambos, I. et al.: Hygroscopic properties of water-soluble matter and humic-like organics in atmospheric fine aerosol, Atmos. Chem. Phys., 4, 35–50, 2004, http://www.atmos-chem-phys.net/4/35/2004/.
Hameri, K., Charlson, R., and Hansson, H. C.: Hygroscopic Properties of Mixed Ammonium Sulfate and Carboxylic Acids Particles, AIChE Journal, 48, 6, 1309–1316, 2002.
Intergovernmental Panel on Climate Change (IPCC): Fourth Assessment Report, Working Group I Report "The Physical Science Basis", Chapter 2, http://www.ipcc.ch/, 2007.
Jacobson, M. C., Hansson, H. C., Noone, K. J., and Charlson, R. J.: Organic atmospheric aerosols: Review and state of science, Rev. Geophys., 38(2), 267–294, 2000.
Kanakidou, M., Seinfeld, J H., Pandis, S. N. et al.: Organic aerosol and global climate mod-

elling: a review, Atmos. Chem. Phys., 5, 1053–1123, 2005, http://www.atmos-chem-phys.net/5/1053/2005/.
Krieger, U. K, Colberg, A. C., Weers, U., Koop, T., and Peter, Th.: Supercooling of single H_2SO_4/H_2O aerosols to 158 K: no evidence for the occurrence of the octahydrate, Geophys. Res. Lett., 27, 2097–2100, 2000.
Krieger, U., K., Braun, C.: Light-scattering intensity fluctuations in single aerosol particles during deliquescence, J. Quant. Spectrosc. Radiat. Transfer, 70, 545–554, 2001.
Levien, B. J.: A Physicochemical Study of Aqueous Citric Acid Solutions, J. Phys. Chem., 59, 640–644, 1955.
Marcolli, C., and Krieger, U. K.: Phase Changes during Hygroscopic Cycles of Mixed Organic/Inorganic Model Systems of Tropospheric Aerosols, J. Phys. Chem. A., 110, 1881–1893, 2006.
Marcolli, C., Luo, B., and Peter, T.: Mixing of the organic aerosol fractions: liquids as the thermodynamically stable phases, J. Phys. Chem. A., 108, 2216–2224, 2004.
Middlebrook, A. M., Murphy, D. M., and Thomson, D. S.: Observations of organic material in individual marine particles at Cape Grim during the First Aerosol Characterization Experiment (ACE 1), J. Geophys. Res., 103(D13), 16 475–16 483, 1998.
Murphy, D. M., Cziczo, D. J., Froyd, K. D., et al.: Single-particle mass spectrometry of tropospheric aerosol particles, J. Geophys. Res., 111, D23S32, 2006.
Pant, A., Fok, A., Parson, M. T., Mak J., and Bertram, A. K.: Deliquescence and crystallization of ammonium sulfate-glutaric acid and sodium chloride-glutaric acid particles, Geophys. Res. Lett, 31, L12111, doi:10.1029/2004GL020025, 2004.
Peng, C.; Chan, M. N., and Chan, C. K.: The Hygroscopic Properties of Dicarboxylic and Multifunctional Acids: Measurements and UNIFAC Predictions, Environ. Sci. Technol., 35, 4495–4501, 2001.
Prenni, A. J., De Mott, P. J., and Kreidenweis, S. M.: Water uptake of internally mixed particles containing ammonium sulfate and dicarboxylic acids, Atmos. Environ., 37 (30), 4243–4251, 2003.
Price, P. B.: A habitat for psychrophiles in deep Antarctic ice, PNAS, 97 (3),1247–1251, 2000.
Richardson, C. B.: A stabilizer for single microscopic particles in a quadrupole trap, Rev. Sci. Instrum., 61, 1334–1335, 1990.
Rogge, W. F., Mazurek, M. A., Hildemann, L. M., and Cass, G. R.: Quantification of urban organic aerosols at a molecular level: identification, abundance and seasonal variation, Atmos.

Environ., 27A, 8, 1309–1330, 1993.
Saxena, P., Hildemann, L. M., McMurry, P. H., and Seinfeld, J. H. J.: Organics alter hygroscopic behaviour of atmospheric particles, J. Geophys. Res., 100(D9), 18 755–18 770, 1995.
Semmler, M., Luo, B.P., Koop, T.: Densities of liquid $H^+/NH_4^+/SO_4^{2-}/NO_3^-/H_2O$ solutions at tropospheric temperatures, Atmos. Environ., 40, 467-483, 2006.
Sjogren, S., Gysel, M., Weingartner, E., Baltensperger, U., Cubison, M. J., Coe, H., Zardini, A. A., Marcolli, C., Krieger, U. K., and Peter, T.: Hygroscopic growth and water uptake kinetics of two-phase aerosol particles consisting of ammonium sulfate, adipic and humic acid mixtures, J. Aerosol Sci., 38, 157–171, 2007.
Stokes, R. H., and Robinson, R. A.: Interactions in aqueous nonelectrolyte solutions, solute-solvent equilibria, J. Phys. Chem., 70, 7, 2126–2131, 1966.
Svenningsson, B., Rissler, J., Swietlicki, E., Mircea, M., Bilde, M., Facchini, M. C., Decesari, S., Fuzzi, S., Zhou, J., Mønster, J., and Rosenørn, T.: Hygroscopic growth and critical supersaturations for mixed aerosol particles of inorganic and organic compounds of atmospheric relevance, Atmos. Chem. Phys., 6, 1937–1952, 2006, http://www.atmos-chem-phys.net/6/1937/2006/.
Thomson, W.: On the equilibrium of vapour at a curved surface of liquid, Phil. Mag. 42, 448–452, 1871.
Videen G., Pellegrino P., Ngo D., Videen, J., S., Pinnick, R., G.: Light-scattering intensity fluctuations in microdroplets containing inclusions. Appl. Opt., 36, 6115–6118, 1997.
Weingartner, E., Gysel, M., and Baltensperger, U.: Hygroscopicity of aerosol particles at low temperatures. 1. New low-temperature H-TDMA instrument: Setup and first applications, Env. Sci. Tech., 36, 1, 55–62, 2002.
Wise, M., E., Surratt, J., D., Curtis, D., B., Shilling, J., E., and Tolbert, M., A.: Hygroscopic growth of ammonium sulfate/dicarboxylic acids, J. Geophys. Res., 108 (D20), 4638, 2003.
Zdanovskii, A. B., Novyi metod rascheta rastvorimostei elektrolitov v mnogokomponentnykh sistemakh 1,2, Zh. Fiz. Khim., 22, 1486–1495, 1478–1485, 1948.

Table 1. Substances used in the experiments.

Substances	Purity	ρ (g/cm^{-3})	M (g/mol)	Producer	Product n°
Ammonium Sulfate	99.99%	1.77	132.14	Aldrich	431540
Citric Acid	≥ 99.5%	1.665	192.027	Fluka	27488
Glutaric Acid	99%	1.424	132.12	Aldrich	U05447-124
Adipic Acid	≥ 99.5%	1.362	146.14	Fluka	09582

Table 2. Summary of the hygroscopicity cycles for the AS:AA=1:3 system (interval and averaged values for 25 cycles and 9 different particles): relative humidity of the pre-deliquescence onset and maximum, RH_0 and RH_m; mass growth factor at the maximum of pre-deliquescence, $g(RH_m)$; DRH; growth factor at DRH, g(DRH); efflorescence of ammonium sulfate, ERH.

RH_0	RH_m	$g(RH_m)$	DRH	g(DRH)	ERH
43–53%, 48.1%	52–65%, 58%	1.03–1.19, 1.10	78–83%, 80.5%	1.16–1.45, 1.37	33-69%, 53%

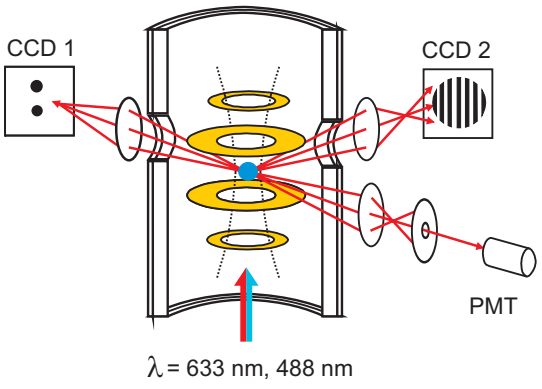

Fig. 1. Schematic of the electrodynamic balance. A three-wall glass chamber hosts four metal rings which supply the electric field needed for particle levitation. The particle is illuminated by two laser beams from below. The scattered light is collected in the near and far field view by two CCD cameras, and its intensity monitored by a photomultiplier (PMT).

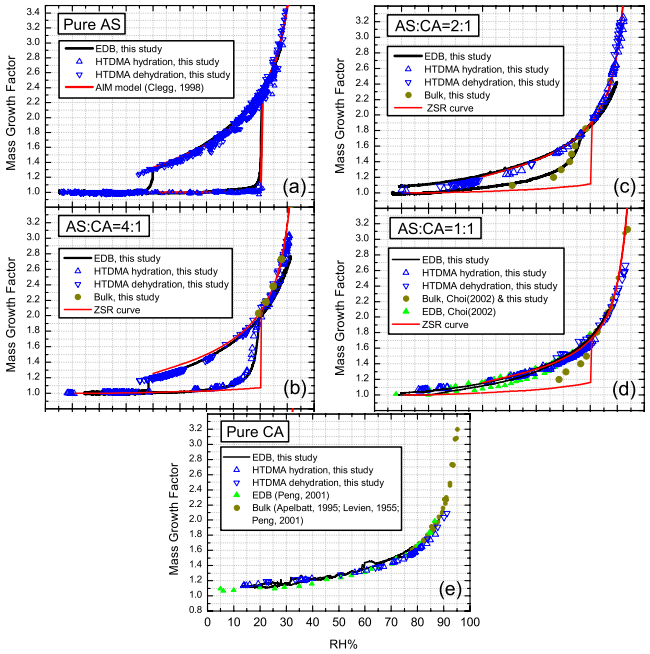

Fig. 2. Hygroscopicity cycles of pure ammonium sulfate (AS) and citric acid (CA) particles (panel **a** and **e**), and mixtures of AS and CA with different molar ratios (4:1, 2:1, 1:1, from panel **b** to panel **d**). Pure AS exhibits hysteresis with distinct deliquescence and efflorescence at RH≈80% and RH=35%-40%. Pure CA particles, instead, are always liquid and absorb and desorb water according to RH changes at any given RH. In the 4:1 case the water uptake becomes apparent at RH≈60%, the DRH and ERH are slightly decreased (2% and 3%, respectively) compared to the pure AS case. The 2:1 case exhibits different behavior for particles in HTDMA (always liquid) and the particle freshly injected at dry conditions in the EDB (solid AS present at dry conditions during hydration) with bulk points very close to the hydration branch of EDB measurements. In the 1:1 mixture the presence of CA in the 1:1 mixture suppresses the hysteresis of AS in both EDB and HTDMA cycles, and particles are always in liquid state.

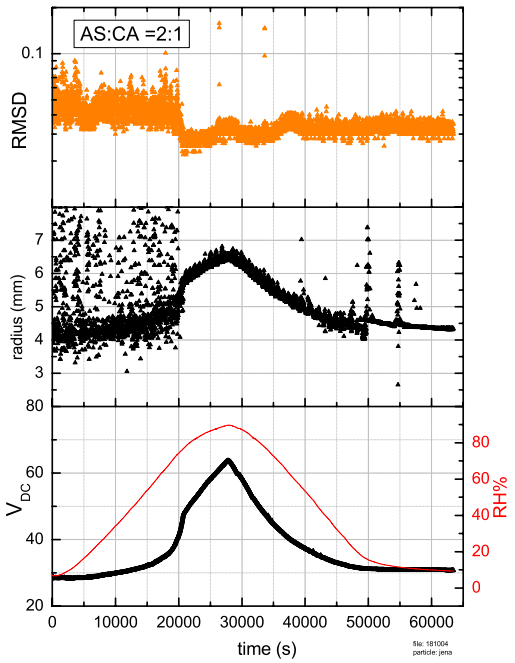

Fig. 3. Time evolution of the hygroscopicity cycle of a single AS/CA particle with 2:1 molar ratio in the EDB. The uppermost panel shows the RMSD of scattered light indicating AS deliquescence at $t \approx 20$ ks. Thereafter, the particle remains liquid without AS efflorescence reoccurring. The middle panel shows the radius calculated by means of the Mie phase functions (as explained in the experimental section). When the particle is not a homogeneous sphere ($t \leq 20$ ks), the phase function allows to derive only a coarse estimate. The lowermost panel was used to construct the humidogram in Fig. 2, panel **(c)**.

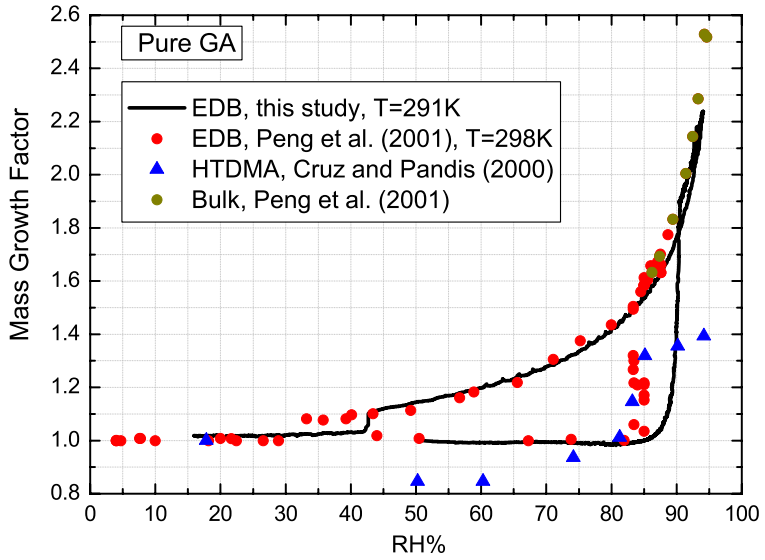

Fig. 4. Hygroscopicity cycles of pure GA particles (cycle time ≈19 h). GA exhibits hysteresis with distinct DRH and ERH. Literature HTDMA data do not fit the bulk data, but show a lower hydration branch likely due to evaporation of the particle during measurements as already noted by Cruz and Pandis (2000).

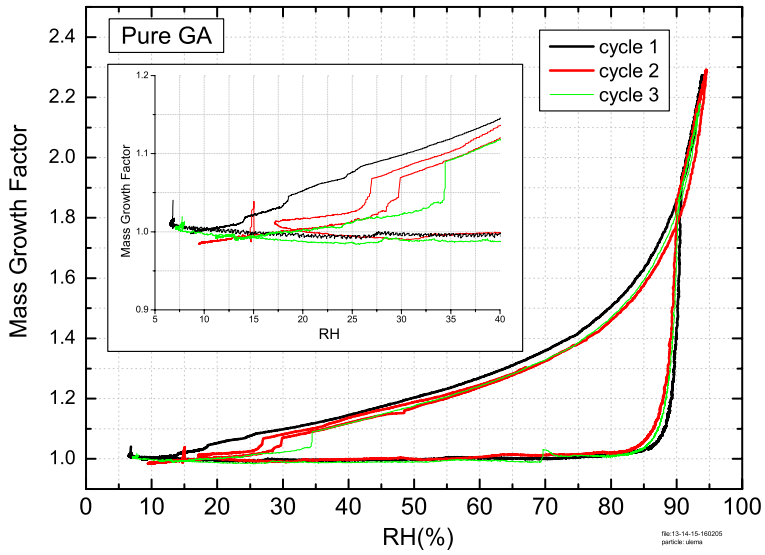

Fig. 5. Consecutive hygroscopicity cycles of a pure GA particle in the EDB. Inset: zoom on ERH showing that crystallization of GA has a low degree of reproducibility (in contrast to AS), ranging from gradual water release to a sharp efflorescence. This can lead to the presence of water also at very dry conditions.

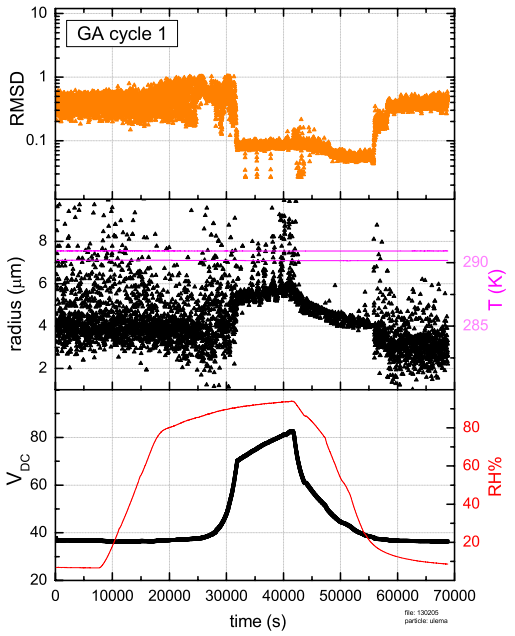

Fig. 6. Hygroscopicity cycle of a pure GA particle in the EDB. The light intensity fluctuations in the uppermost panel show a clear deliquescence ($t \approx 32$ ks, RH≈90.5%) and efflorescence ($t \approx 55$ ks, RH≈18%), proving that the particle changes its phase from liquid to crystalline with no evident mass change (lowermost panel). The optical radius evolution is plotted in the middle panel and is an indirect indication of a liquid particle in the region 32 ks$\leq t \leq$55 ks. The lowermost panel was used to construct the humidogram in Fig. 5, black curve, where no efflorescence would have been detected solely based on mass measurements.

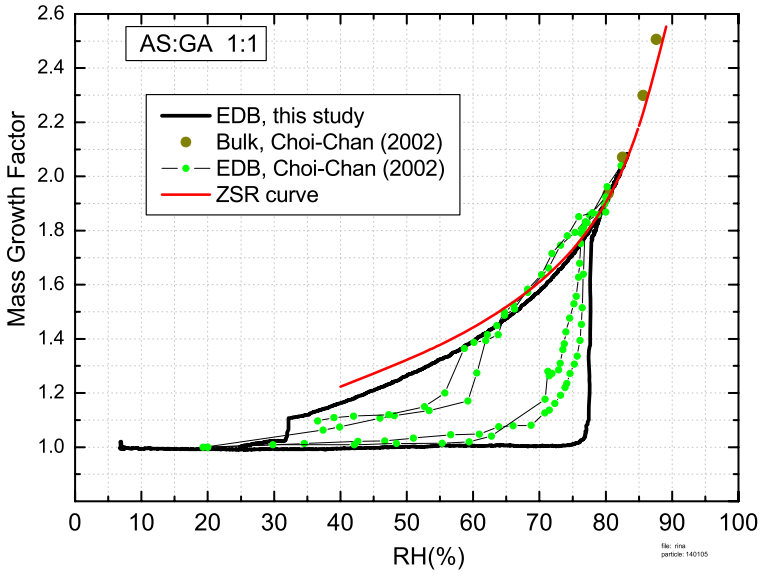

Fig. 7. Hygroscopicity cycle of AS/GA particles, 1:1 molar ratio. DRH and ERH points are lower compared to pure AS by 3% and 8%, respectively. DRH is lower than both deliquescence of pure AS and pure GA. ERH of GA is now triggered by the presence of AS.

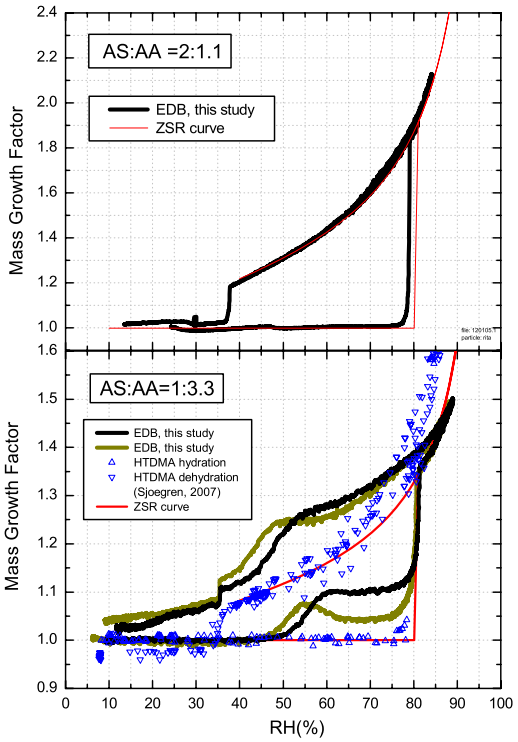

Fig. 8. Hygroscopicity cycles of AS/AA particles in the EDB; 2:1.1 molar ratio (upper panel) and 1:3.3 molar ratio (lower panel). The 2:1.1 case resembles the pure AS behavior, while there are modified hydration and dehydration branches in the 1:3.3 case which strongly differ from ZSR predictions. Non-monotonous mass changes must be due to structural changes (particle compaction) occurring during water uptake.

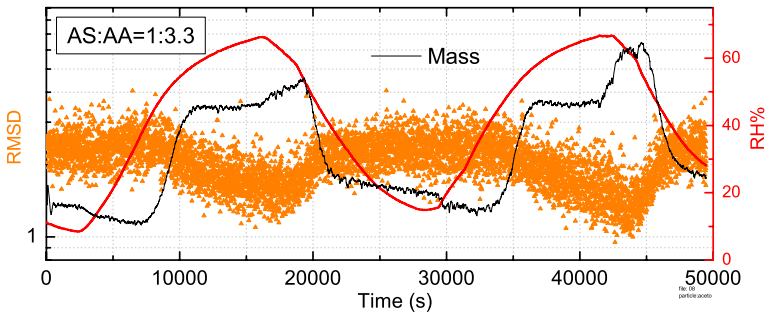

Fig. 9. Two incomplete consecutive cycles of an AS/AA particle, 1:3.3 molar ratio. Light intensity fluctuations (orange symbols) are in phase opposition with the mass and ambient RH (black and red curves, respectively), indicating that the pre-deliquescence water uptake described in the lower panel of Fig. 8 is reversible.